Synaptic Activation of Voltage-Gated Channels in the Dendrites of Hippocampal Pyramidal Neurons

Jeffrey C. Magee and Daniel Johnston

Activation of dendritic voltage-gated ion channels by local synaptic input was tested by simultaneous dendrite-attached patch-clamp recordings and whole-cell somatic voltage recordings made from CA1 pyramidal neurons in hippocampal slices. Schaffer collateral stimulation elicited subthreshold excitatory postsynaptic potentials (EPSPs) that opened voltage-gated sodium and calcium channels in the apical dendrites. The EPSP-activated sodium channels opened near the peak of the EPSP, whereas low voltage–activated calcium channels opened near the EPSP peak and during the decay phase. Dendritic high voltage–activated channels required somatic action potential generation or suprathreshold synaptic trains for activation. Dendritic voltage-gated channels are, therefore, likely to participate in dendritic integration of synaptic events.

The extensive dendritic arborizations of CA1 pyramidal neurons each receive tens of thousands of widely distributed synaptic inputs, most of which are both physically and electrotonically distant from the soma (*1*). Cable filtering of the synaptic current reduces the amplitude of synaptic potentials and limits spatial summation among distributed synapses, severely diminishing the impact of many synapses on neuronal output (*2*). Active dendritic channels, which occur in a wide variety of central neurons (*3–7*), could amplify the efficacy of electrotonically distant synaptic inputs. CA1 pyramidal neurons have a substantial density of tetrodotoxin (TTX)-sensitive Na^+ channels and both low- and high-threshold Ca^{2+} channels in their apical dendrites (*6, 7*). The voltage-dependent properties of Na^+ and T-type Ca^{2+} channels predict that EPSPs of 10 to 20 mV would activate these channels (*7–9*).

Dendrites of identified pyramidal somata were visually followed into stratum radiatum for distances ranging from 50 to 300 μm from the cell body (*10*). Single Na^+or Ca^{2+} channels were recorded in a dendrite-attached patch configuration, and in many cases simultaneous whole-cell voltage recordings were made from the soma of the neuron under study (Fig. 1A) (*11*). Na^+ channel activity (Fig. 1B) was identified by inward current polarity, voltage-dependent channel gating, and unitary current amplitude (*7*). Channel activity was suppressed by inclusion of TTX (1 M) ($n = 5$) in the recording pipette or by addition of QX-314 (2 mM) ($n = 2$) to the cell interior from the somatic whole-cell electrode. Pipette solutions containing $CdCl_2$ (0.5 mM) ($n = 7$) had no effect on channel activity. Na^+ channels were found in every patch and more than a single channel was always present (range, 2 to 10 per patch). Ca^{2+} channel activity was also identified by inward current polarity, voltage-dependent channel gating, unitary current amplitude, and by single-channel behavior.

At least two distinct types of Ca^{2+} channel activity were encountered regularly on dendrites greater than 100 μm from the soma (*7*). The first type was a low voltage–activated (LVA), small conductance (~9 pS) channel very similar in basic characteristics to the T-type Ca^{2+} channel (Fig. 1C) (*9*). The second type was a high voltage–activated (HVA), moderate conductance (~15 pS) channel that presents a pharma-

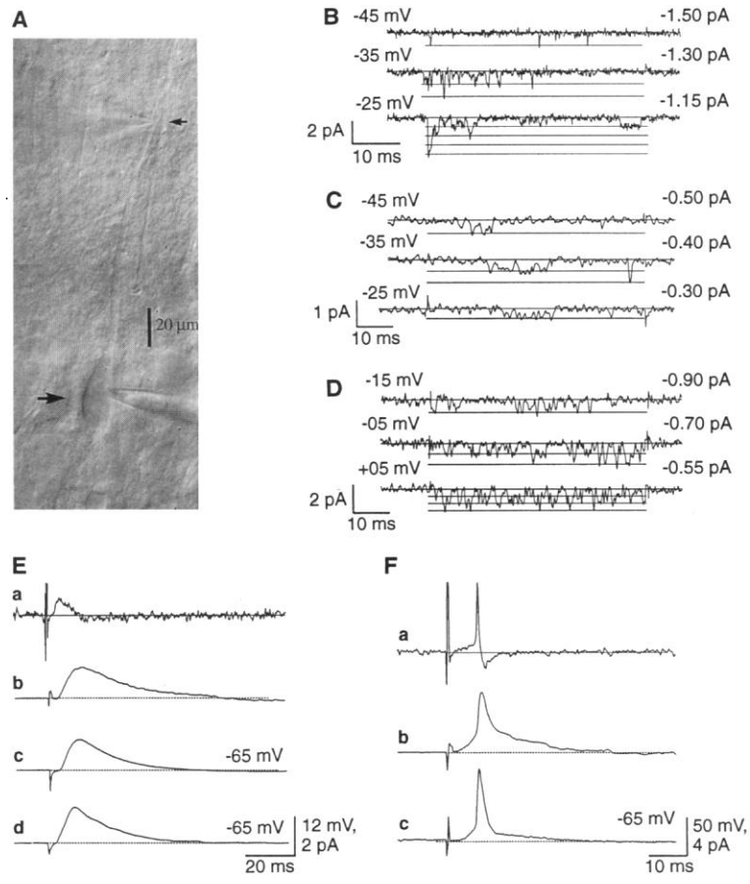

Fig. 1. (**A**) Differential interference contrast image showing a CA1 pyramidal neuron with somatic and dendritic (105 μm from soma; large arrow) recording pipettes. Photos were superimposed, as the dendrite was in a slightly deeper focal plane than the soma. (**B**) Selected sweeps of Na^+ channel activity evoked by step depolarizations from −85 mV. Slope conductance was ~15 pS. (**C**) Selected sweeps of LVA Ca^{2+} channel activity evoked by step depolarizations from −105 mV. Slope conductance was ~9 pS. (**D**) Selected sweeps of HVA Ca^{2+} channel activity evoked by step depolarizations from −65 mV. Slope conductance was ~16 pS. (**E**) Stimulation of Schaffer collaterals evokes several characteristic waveforms depending on the recording mode. (a) Current trace recorded in dendrite-attached configuration in response to subthreshold Schaffer collateral stimulation demonstrating the capacitive current transient evoked by EPSPs. (b) Integral of current trace in (a). Voltage scale bar does not apply to this trace. (c) EPSP recorded simultaneously by a second pipette in whole-cell mode at the soma. (d) EPSP recorded from dendrite after rupture of membrane patch, showing a very similar time course to that of the integral of the current trace recorded in the dendrite-attached configuration. (**F**) Action potential generation also evokes distinctive waveforms. (a) Current trace recorded in the dendrite-attached configuration in response to suprathreshold Schaffer collateral stimulation. (b) Integral of current trace in (a) demonstrating a spike-like waveform. (c) Action potential recorded simultaneously by a second pipette in whole-cell mode at the soma. Records in (B), (C), and (D) have leakage and capacitive currents digitally subtracted by averaging null traces or scaling traces of smaller amplitude. Test potentials and unitary current amplitudes are shown above traces. Records in (C) have been digitally refiltered at 0.5 kHz. All traces in (E) and (F) are the averages of five consecutive traces and are from the neuron shown in (A).

cological profile similar to that reported for R-type Ca^{2+} channels (Fig. 1D) (*7*, *12*). A third type, which was primarily encountered in patches within 100 μm from the soma, had characteristics of the HVA L-type Ca^{2+} channel (*7*, 9). Addition of 0.5 mM $CdCl_2$ (n = 3) to the pipette solution suppressed all Ca^{2+} channel activity, whereas 1 μm TTX (n = 12) in the pipette or 2 mM QX-314 (n = 5) inside the cell were without effect. Calcium channels were found in about 80% of patches examined and more than a single channel was always present (range, 2 to 7 per patch).

EPSPs evoked by stimulation of Schaffer collaterals induced an initial current transient that resembled the first derivative of membrane voltage (dV/dt). Integration of these transients produced waveforms that were nearly identical to EPSPs recorded intracellularly from the dendrite (Fig. 1E). These currents, therefore, appeared to be capacitive currents induced by depolarization of the membrane patch by the evoked EPSP. No leak current was induced. EPSPs of sufficient amplitude generated action potentials, which also induced distinctive capacitive currents (Fig. 1F).

EPSPs below action potential threshold consistently activated Na^+ channels located within the CA1 dendrite-attached patch (n = 15) (Fig. 2A). With TTX present in the pipette (n = 3), there was no EPSP-associated channel activity in dendritic patches. Most channel openings were near the peak of the EPSP, but occasional openings were encountered during either the rising or falling phases of the EPSP. Both early transient and later occurring prolonged channel activity were evoked by the EPSPs (Fig. 2B). Channel openings were observed about every third synaptic stimulation when EPSPs of 15 to 20 mV (as recorded from the dendrite under study) were evoked. In general, higher amplitude EPSPs also opened Na^+ channels, but these EPSPs were sufficient to generate somatic action potentials. Occasionally, synchronous activation of a large proportion of Na^+ channels in the patch was recorded (Fig. 2C) from patches in the distal dendritic regions (>200 μm), where large dendritic EPSPs (amplitude 25 mV) could be generated that remained subthreshold at the somatic region. Holding the membrane patch 10 mV depolarized from resting membrane potential (V_m) also facilitated the synchronous activation of Na^+ channels (Fig. 2C). Plots of unitary current amplitude versus approximate membrane potential (I-V) revealed that the slope conductance (16 ± 1.0 pS; n = 8) and reversal potential (+56 ± 1 mV; n = 8) of EPSP-activated channel openings were similar to those calculated from step depolarizations in the same patches and for other neuronal Na^+ channels (Fig. 2, C and D) (*13*).

Schaffer collateral stimulation also opened single Ca^{2+} channels in dendrite-attached patches (n = 12) (Fig. 3A). $CdCl_2$ (0.5 mM) in the pipette (n = 3) blocked this activity. Single-channel openings of LVA Ca^{2+} channels were most often observed near the peak or falling phases of the EPSPs (Fig. 3A). EPSP-activated channel openings displayed the small unitary current amplitude and slope conductance (9 ± 1.6 pS) (n = 6) characteristic of dendritic LVA Ca^{2+} channels (Fig. 3B) (*7*, 9). EPSPs with a peak amplitude of 10 mV (at the site of recording) were necessary for activation of LVA Ca^{2+} channels, whereas just-subthreshold EPSPs (20 to 25 mV at the site of recording) activated LVA channels with near maximal fractional open time (NP_o). In several patches we explored the amount of steady-state inactivation of these channels near rest. From a holding potential of 10 to 15 mV depolarized from rest [to counter charge screening by the 20 mM Ba^{2+} solution in the pipette (*14*)], EPSP-activated LVA channel activity was relatively infrequent (Fig. 3C). A 4-s hyperpolarizing prepulse 400 ms before synaptic stimulation increased the NP_o of Ca^{2+} channels in a voltage-

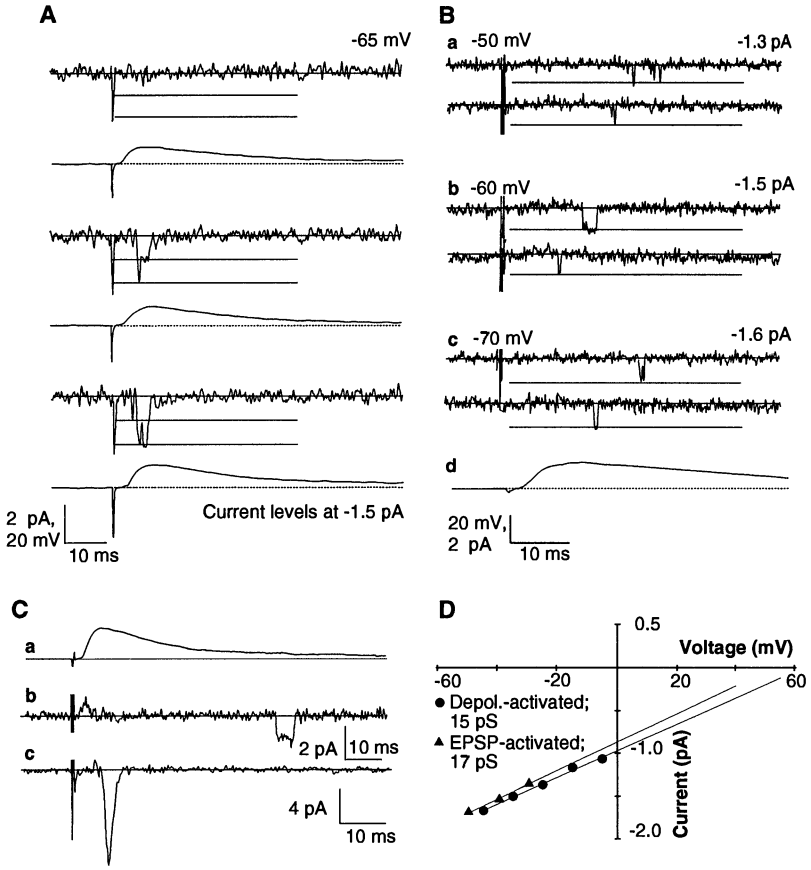

Fig. 2. Na^+ channel openings are evoked by subthreshold EPSPs. (**A**) Consecutive sweeps of dendrite-attached patch recordings (top traces) showing Na^+ channel activation by EPSPs and somatic voltage simultaneously recorded by a second whole-cell electrode (bottom traces). (**B**) Na^+ channel activity evoked by intracellular EPSPs from another dendrite showing unitary current amplitudes recorded when the patch was held (a) 15 mV depolarized, (b) 5 mV depolarized, and (c) 5 mV hyperpolarized of V_m. (d) Average of five EPSPs recorded from the dendrite immediately after rupture of the patch. (**C**) Synaptic stimulation induces both late prolonged and initial transient Na^+ channel activity. (a) Integral of EPSP-induced capacitive current showing the EPSP time course. (b) Dendrite-attached patch recording showing activation of late prolonged Na^+ channel activity. (c) Dendrite-attached patch recording showing synchronous activation of six of at least nine Na^+ channels present in the dendritic patch. (**D**) I-V curves of Na^+ channel openings evoked by depolarizations of the patch by voltage steps or by intracellular EPSPs [same dendrite as in (B)]. EPSP-activated channel openings display a slope conductance and reversal potential characteristic of Na^+ channels. The voltage of EPSP activation is corrected for average EPSP amplitude as recorded after rupture of the membrane patch. V_m = −65 mV; EPSP amplitude (average of five traces) = 20 mV. Voltages displayed above records in (A) and (B) are patch holding potentials. The initial capacity current has been subtracted from the dendrite-attached patch recordings by the average of traces with no channel activity. Records in (A) and (C) were filtered at 1 kHz, whereas those in (B) were filtered at 2 kHz. Dendrite-attached recordings are from 120 (A), 180 (B), and 290 μm (C) from the soma.

Division of Neuroscience, Baylor College of Medicine, Houston, TX 77030, USA.

dependent manner (n = 4) (Fig. 3, C and D). This result suggests that a large proportion of the LVA channel population is inactivated at resting V_m and that membrane hyperpolarization, and subsequent channel deinactivation, are necessary for maximal channel activation by EPSPs. Thus, the contribution of LVA Ca^{2+} channels to EPSP amplitude and kinetics and Ca^{2+} influx would be particularly enhanced for EPSPs occurring after hyperpolarizing IPSPs or spike-mediated afterhyperpolarizations.

Subthreshold synaptic stimulation was not sufficient to open dendritic HVA Ca^{2+} channels. Instead, somatically generated action potentials or trains of suprathreshold synaptic stimulation were required for HVA channel activation (Fig. 4, A and B). The transient single-channel openings and frequent reopenings of dendritic HVA Ca^{2+} channels (both L- and putative R-type) were observed during and after the repolarization phase of somatically generated action potentials. Such channel openings displayed a slope conductance (15 to 25 pS) associated with dendritic HVA Ca^{2+} channels (Fig. 4B). Hyperpolarizing prepulses had no effect on the synaptic activation of HVA Ca^{2+} channels. These observations suggest that dendritic HVA Ca^{2+} channels provide an influx of Ca^{2+} into the apical dendrites in response to action potential generation and it appears that CA1 pyramidal dendrites contain two functionally distinct populations of Ca^{2+} channels.

These results demonstrate that EPSPs can open dendritic Na^+ and LVA Ca^{2+} channels in dendrites. Prior hyperpolarization should enhance the EPSP activation of LVA channels, although the relatively unphysiological conditions of our experiments

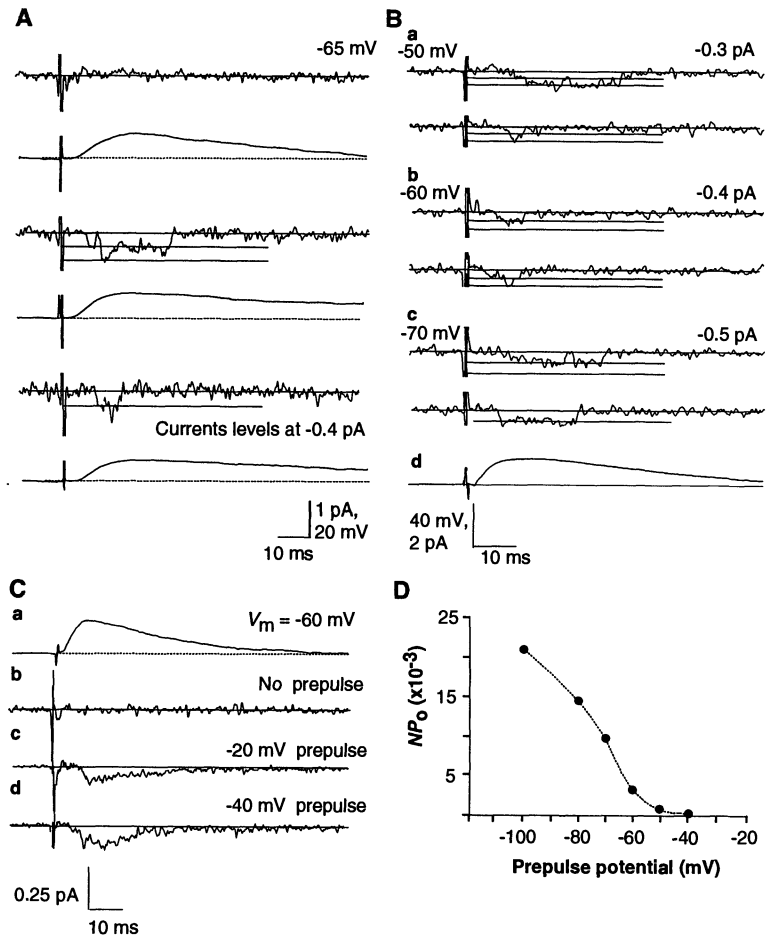

Fig. 3. Subthreshold synaptic activation of LVA Ca^{2+} channels. (**A**) Consecutive sweeps of dendrite-attached patch recordings with patch held at V_m (top traces) showing Ca^{2+} channel activation by subthreshold EPSPs. Bottom traces are somatic voltage simultaneously recorded by a second whole-cell electrode. (**B**) Dendrite-attached patch recordings demonstrating the voltage dependence of EPSP-activated unitary current amplitudes, when the patch is held (a) 15 mV depolarized, (b) 5 mV depolarized, and (c) 5 mV hyperpolarized of V_m. Two traces containing openings were selected from consecutive sweeps and illustrated for each voltage. Slope conductance of EPSP-evoked channel activity was 10 pS, compared with 8 pS when activated by voltage steps. (d) Average of five EPSPs recorded from the dendrite immediately after rupture of patch. (**C**) Hyperpolarizing prepulses increase the EPSP activation of LVA Ca^{2+} channels. (a) Integral of EPSP-induced capacitive current showing EPSP time course. (b) Ensemble average of 50 consecutive current traces showing minimal EPSP channel activation without prepulse. (c) Ensemble average of 60 consecutive current traces showing increased EPSP channel activation after a 4-s prepulse of −20 mV. (d) Ensemble average of 60 consecutive current traces showing maximal EPSP channel activation after a 4-s prepulse of −40 mV. The patch was returned to a holding potential that was 10 mV depolarized from V_m 400 ms before synaptic stimulation. (**D**) Plot of maximal fractional open time (NP_o) for EPSP-activated LVA Ca^{2+} channel activity versus prepulse amplitude. Note that this voltage range is similar to that reported for steady-state inactivation of LVA Ca^{2+} channels (*7*, *9*). Voltages displayed above records in (A) and (B) are patch holding potentials. The initial capacity current has been subtracted as in Fig. 2. Traces in (B) and (C) were digitally refiltered at 0.5 kHz. Recordings in (A), (B), and (C) are 260, 120, and 150 μm from the soma, respectively. NP_o was calculated as in (*7*).

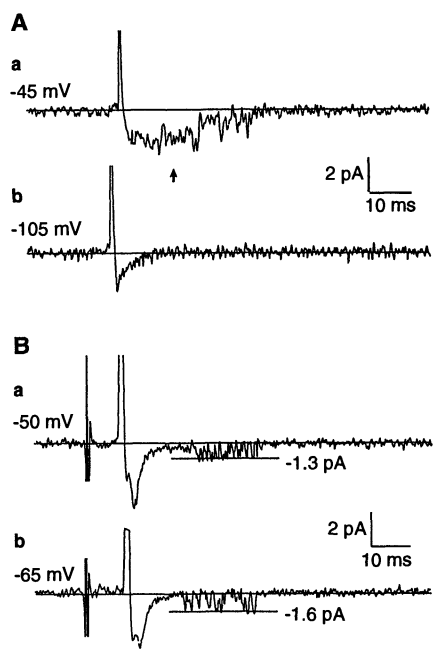

Fig. 4. Activation of dendritic HVA Ca^{2+} channels. (**A**) Somatically generated action potentials open dendritic HVA Ca^{2+} channels. (a) Dendrite-attached patch recording of action potential activation of many Ca^{2+} channels (arrow). The patch contained at least seven L- and R-type Ca^{2+} channels, and the membrane patch was held 20 mV depolarized of resting V_m. (b) With the membrane patch held 40 mV hyperpolarized from resting V_m, no channels were opened, and the somatic action potential induced only a capacitive current. Somatic action potentials were initiated by a 0.5-ms current injection from a second whole-cell pipette. (**B**) Channels opened by action potentials have large unitary current amplitudes and moderate to high slope conductances. Dendrite-attached recordings showing HVA Ca^{2+} channel activation by synaptically evoked action potentials with the membrane patch held 15 mV depolarized of V_m (a) and at V_m (b). Slope conductance of these channels was ~17 pS, which is similar to that found for R-type Ca^{2+} channels (see Fig. 1D). Recordings in (A) and (B) are 50 and 110 μm from the soma, respectively.

may have accentuated this effect. The activation of dendritic Na^+ channels does not necessarily lead to fully overshooting action potentials but may simply elevate EPSP amplitude. The slow kinetics of LVA Ca^{2+} currents, and possibly persistent Na^+ currents, could also extend EPSP duration, prolonging the time available for synaptic integration (*2*, *15*). Dendritic Na^+ and Ca^{2+}channels are therefore capable of enhancing the efficacy of more distal and widely distributed synaptic contacts by increasing both the strength and duration of synaptic input over that predicted by the passive cable properties of the neuron.

Activation of voltage-gated Na^+ and Ca^{2+} channels in dendrites may also provide an important local signal for dendritic integration of synaptic inputs. Subthreshold synaptic activation of dendritic voltage-gated channels could have very localized effects on the membrane time constant, local ionic driving forces, ligand-gated channel conductances, and the influx of Ca^{2+}. Such local events, perhaps confined to the specific dendritic branch where synaptic input occurs, could affect the spatial and temporal summation of synaptic inputs occurring in that region and would provide a limited space in which Ca^{2+}-dependent intracellular events can take place (*16*). Subthreshold synaptic activation of dendritic channels may provide mechanisms for highly localized, short- or long-duration modifications in the process of synaptic integration.

In contrast, our results demonstrate directly that Ca^{2+} channels are opened by action potentials backpropagating into the dendrites, as has been suggested with fluorescence imaging (*6*). We demonstrate that rises in intracellular Ca^{2+} are due, at least in part, to the opening of HVA Ca^{2+} channels. The opening of these channels can occur tens of milliseconds after the action potential (Fig. 4B) and may be related to the repolarization openings described for HVA Ca^{2+} channels (*17*). Activation of the larger conductance HVA Ca^{2+} channels will provide an influx of Ca^{2+} throughout an extended portion of the dendritic arborization (defined by the extent of action potential propagation). The spatial domain of the effects of these channels will therefore be much more extensive compared with their effects after subthreshold activation. Thus, the voltage-gated channels in CA1 apical dendrites may modify synaptic strength over either localized or broad areas of the dendrites (*18*).

REFERENCES AND NOTES

1. P. Andersen, M. Raastad, J. F. Storm, *Cold Spring Harbor Symp. Quant. Biol.* **55**, 81 (1990); K. M. Harris, F. E. Jensen, B. Tsao, *J. Neurosci.* **12**, 2685 (1992).
2. S. W. Jaslove, *Neuroscience* **47**, 495 (1992); N. Spruston, D. Jaffe, S. H. Williams, D. Johnston, *J. Neurophysiol.* **70**, 781 (1993); N. Spruston, D. Jaffe, D. Johnston, *Trends Neurosci.* **17**, 161 (1994).
3. R. E. Westenbroek, M. K. Ahlijanian, W. A. Catterall, *Nature* **347**, 281 (1990); R. Llinas, M. Sugimori, D. E. Hillman, B. Cherksey, *Trends Neurosci.* **15**, 351 (1992); R. E. Westenbroek *et al.*, *Neuron* **9**, 1099 (1992).
4. H. Markram and B. Sakmann, *Proc. Natl. Acad. Sci. U.S.A.* **91**, 5207 (1994).
5. M. M. Usowicz, M. Sugimori, R. Llinas, *Neuron* **9**, 1185 (1992); G. J. Stuart and B. Sakmann, *Nature* **367**, 69 (1994).
6. H. Miyakawa *et al.*, *Neuron* **9**, 1163 (1992); B. R. Christie, L. S. Elliot, H. Miyakawa, K. Ito, D. Johnston, *J. Neurophysiol.*, in press; D. Jaffe *et al.*, *Nature* **357**, 244 (1992).
7. J. C. Magee and D. Johnston, *J. Physiol. (London)*, in press.
8. P. Sah, A. J. Gibb, P. W. Gage, *J. Gen. Physiol.* **91**, 373 (1988); N. Ogata and H. Tatebayashi, *Pflügers Arch.* **416**, 594 (1990).
9. R. E. Fisher, R. Gray, D. Johnston, *J. Neurophysiol.* **64**, 91(1990); D. J. Mogul and A. P. Fox, *J. Physiol. (London)* **433**, 259 (1991); T. J. O'Dell and B. E. Alger, *ibid.* **436**, 739 (1991).
10. Hippocampal slices (400 μm) were prepared from 5- to 8-week-old Sprague-Dawley rats according to standard procedures, and individual neurons were viewed as described [G. J. Stuart, H. U. Dodt, B. Sakmann *Pflügers Arch.* **423**, 511 (1993)]. The external solution contained 124 mM NaCl, 2.5 mM KCl, 1.2 mM $NaPO_4$, 26 mM $NaHCO_3$, 2.0 mM $CaCl_2$, 1.0 mM $MgCl_2$, and 20 mM dextrose and was bubbled with 95% O_2, 5% CO_2 at ~22°C.
11. Somatic voltage was recorded with an Axoclamp 2A amplifier (Axon Instruments) in "bridge" mode. Whole-cell recording pipettes (2 to 4 megohms) were filled with 140 mM $KMeSO_4$, 10 mM Hepes, 0.5 mM EGTA, 3.0 mM $MgCl_2$, 4.0 mM sodium adenosine triphosphate, and 0.1 mM tris–guanosine triphosphate (pH 7.4 with KOH). For Na^+ channel recordings, pipettes (6 to 10 megohms) contained 110 mM NaCl, 30 mM tetraethylammonium chloride (TEACl), 10 mM Hepes, 2.0 mM $CaCl_2$, and 5 mM 4-aminopyridine (pH 7.4 with TEAOH). Na^+ channel records were analog filtered at 2 kHz (−3 db; 8-pole Bessel) and digitized at 20 kHz. For Ca^{2+} channel recordings, the pipette solution contained 20 mM $BaCl_2$, 110 mM TEACl, 10 mM Hepes, 5 mM 4-aminopyridine, and 1 μM TTX (pH 7.4 with TEAOH). Ca^{2+} channel records were analog filtered at 2 or 1 kHz and digitized at 10 kHz. For single-electrode recordings, V_m (−60 to −70 mV) was determined by later rupture of the patch to whole-cell recording mode. For focal extracellular stimulation, a glass pipette (tip diameter 10 μm) or a single-etched platinum wire (tip diameter <5 μm) was placed near the dendrite under study.
12. P. T. Ellinor *et al.*, *Nature* **32**, 455 (1993); J. F. Zhang *et al.*, *Neuropharmacology* **363**, 1075 (1993); T. Schneider *et al.*, *Biophys. J.* **66**, A423 (1994).
13. E. M. Fenwick, A. Marty, E. Neher, *J. Physiol. (London)* **331**, 599 (1982); C. Alzheimer, P. C. Schwindt, W. E. Crill, *J. Neurosci.* **13**, 660 (1993).
14. B. Hille, *Ionic Channels of Excitable Membranes* (Sinauer, Sunderland, MA, 1992).
15. R. D. Traub and R. Llinas, *J. Neurophysiol.* **42**, 476 (1979); R. A. Deisz, G. Fortin, W. Zieglgansberger, *ibid.* **65**, 371 (1991).
16. G. White, W. B. Levy, O. Steward, *ibid.* **64**, 1186 (1990); D. B. Jaffe *et al.*, *ibid.* **71**, 1065 (1993).
17. R. E. Fisher, R. Gray, D. Johnston, *ibid.* **64**, 91 (1990); O. Thibault, N. M. Porter, P. W. Landfeld, *Proc. Natl. Acad. Sci. U.S.A.* **90**, 11792 (1993).
18. D. Johnston, W. Williams, D. Jaffe, R. Gray, *Annu. Rev. Physiol.* **54**, 489 (1992); D. M. Kullmann, D. J. Perkel, T. Manabe, R. Nicoll, *Neuron* **9**, 1175 (1992).

19. We thank C. Colbert for comments on the manuscript. Supported by NIH grants NS09482, NS11535, MH44754, and MH48432.

5 December 1994; accepted 16 February 1995

Silver as a Probe of Pore-Forming Residues in a Potassium Channel

Qiang Lü and Christopher Miller*

In voltage-dependent potassium channels, the molecular determinants of ion selectivity are found in the P (pore) region, a stretch of 21 contiguous residues. Cysteine was introduced at each P region position in a Shaker potassium channel. Residues projecting side chains into the pore were identified by means of channel inhibition by a sulfhydryl-reactive potassium ion analog, silver ion. The pattern of silver ion reactivity contradicts a β barrel architecture of potassium channel pores.

Voltage-gated ion channels of excitable cell membranes operate as expert inorganic chemists. K^+ channels, for instance, discriminate well among the alkali metal cations; in some cases they transport K^+ 1000 times more efficiently than Na^+ (*1*). Because ions traverse channel proteins by diffusion through narrow, water-filled pores, questions of ion selectivity have focused on the nature of the chemical groups that line these pores. In voltage-gated K^+ channels, the selectivity-determining groups reside in the P region, a conserved hairpin sequence that enters and leaves the membrane from the extracellular side (*2–4*). Other transmembrane sequences contribute to the cytoplasmic end of K^+ channel pores (*5*), but residues that strongly affect ion selectivity have been found only in the P region. K^+ channels are tetrameric, with P regions of the four subunits symmetrically surrounding the conduction pathway (*6–8*), but the chemistry of K^+ ligation within the pore is unknown (*9*). To ascertain which residues project side chains into the pore lumen, we used cysteine susceptibility analysis (*10*), in which individual residues in the pore-forming sequence are mutated to cysteine and the sensitivity of the resulting channels to

Howard Hughes Medical Institute and Graduate Department of Biochemistry, Brandeis University, Waltham, MA 02254, USA.

*To whom correspondence should be addressed.